*This is the peer reviewed version of the following article: F. Schendzielorz et al., Angew. Chem. Int. Ed., **2019**, 58, 830-834, which has been published in final form at* **DOI**: 10.1002/anie.201812125*. This article may be used for non-commercial purposes in accordance with Wiley Terms and Conditions for Use of Self-Archived Versions.*

Metal-Ligand Cooperative Synthesis of Benzonitrile via Electrochemical Reduction and Photolytic Splitting of Dinitrogen

Florian Schendzielorz,[a] Markus Finger,[a] Josh Abbenseth,[a] Christian Würtele,[a] Vera Krewald,*[b] and Sven Schneider*[a]

Dedicated to Prof. Dr. F. Tuczek on the occasion of his 60th birthday

Abstract: Thermal nitrogen fixation relies on strong reductants to overcome the extraordinarily large N–N bond energy. Photochemical strategies that drive N_2 fixation are scarcely developed. Here, the synthesis of a dinuclear N_2-bridged complex is presented upon reduction of a rhenium(III) pincer platform. Photochemical splitting into terminal nitride complexes is triggered by visible light. Clean *N*-transfer with benzoyl chloride to free benzamide and benzonitrile is enabled by cooperative $2H^+/2e^-$ transfer of the pincer ligand. A three-step cycle is demonstrated for N_2 to nitrile fixation that relies on electrochemical reduction, photochemical N_2-splitting and thermal *N*-transfer.

The Haber-Bosch process consumes large amounts of energy, for the generation of H_2. Electrocatalytic N_2 reduction has therefore been targeted as an attractive alternative.[1,2] Nitrogen fixation at ambient conditions with molecular catalysts has seen remarkable progress,[3] in some cases also for electrochemical ammonia generation.[4] The direct synthesis of other compounds than NH_3 from N_2 remains a formidable challenge. Catalytic protocols are only known for trisilylamine.[5] Nitriles,[6,7,8] isocyanates,[9] silylamines,[10,11] and borylamines,[12] have been synthesized within stoichiometric, cyclic reaction sequences that allow for evaluating strategies to offset the extremely strong N≡N bond (225 kcal/mol), enable E–N (E = C, Si, B) bond formation and deliver six reduction equivalents. All reported 'synthetic cycles' proceed through initial N_2 cleavage into nitride complexes. Subsequent *N*-transfer typically requires strong electrophiles like alkyl triflates. The thermochemistry of N_2 splitting must therefore be tuned to avoid nitride overstabilization and enable functionalization with reagents that are more compatible with reductive conditions.

We have examined N_2 activation and splitting, i.e. triggered by chemical or electrochemical reduction of pincer halide complexes.[13,14] The rhenium(III) precursor [$ReCl_2$(PNP^{tBu})] (**1**; PNP^{tBu} = $N(CH_2CH_2P\,t\!Bu_2)_2$) exhibits a complex mechanism via rapid Re^{III}/Re^{II}-reduction, N_2-binding, halide loss, Re^{II}/Re^{I}-reduction and Re^{I}/Re^{III}-comproportionation.[13b] Splitting of the resulting dinuclear complex [(μ-N_2){ReCl(PNP^{tBu})}$_2$] (**2**) is rate-determining and gives the nitride complex [ReNCl(PNP^{tBu})] (**3**). A simple electronic structure model for the Re–N–N–Re core of key intermediate **2** ($\pi^{10}\delta^4$-configuration; Scheme 1) provides a starting point to tune the thermochemistry.[15] We now report a modified platform that splits N_2 photolytically into more reactive nitrides that can be transferred with benzoyl chloride. The pincer ligand serves as $2e^-/2H^+$ reservoir, enabling electrochemical N_2 reduction, photochemical splitting and thermal transfer within a three-step cycle.

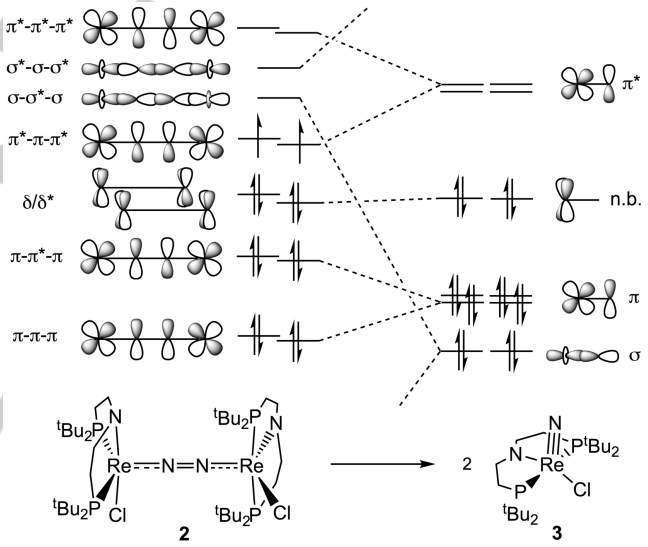

Scheme 1. Schematic frontier orbital correlation diagram for the splitting of N_2-bridged complex **2** into two nitrides **3** (n.b. = non bonding).[13b,15]

The Re^{III} complex [$ReCl_3$(*H*PNP^{iPr})] (**4**) was obtained in 70 % isolated yield.[16] In contrast to **1**, the amide complex [$ReCl_2$(PNP^{iPr})] could not be isolated in analytical purity. **4** displays strongly shifted NMR resonances, as exemplified by the $^{31}P\{^1H\}$-NMR signal (δ_P = -1525.9 ppm). However, the sharp signals exhibit well-resolved *J*-coupling. This observation can be rationalized with a magnetic, energetically isolated ground state that results from excited state admixture via spin-orbit coupling. Contributions from temperature independent paramagnetism (TIP) are well documented for 3rd row complexes with d^4 (octahedral Re^{III}, Os^{IV}) and d^6 configuration (square-planar, Os^{II}).[17] Single-crystal X-ray diffraction confirmed meridional coordination of the neutral diphosphinoamine ligand (Figure 1a).

[a] M. Sc. F. Schendzielorz, Dr. Markus Finger, M. Sc. J. Abbenseth, Dr. C. Würtele, Prof. Dr. S. Schneider
Georg-August-Universität
Institut für Anorganische Chemie
Tammannstrasse 4, 37077 Göttingen (Germany)
E-mail: sven.schneider@chemie.uni-goettingen.de
[b] Dr. Vera Krewald
Department of Chemistry
University of Bath
Claverton Down, Bath BA2 7AY, United Kingdom

Supporting information for this article is given via a link at the end of the document.

*This is the peer reviewed version of the following article: F. Schendzielorz et al., Angew. Chem. Int. Ed., **2019**, 58, 830-834, which has been published in final form at* **DOI**: 10.1002/anie.201812125. *This article may be used for non-commercial purposes in accordance with Wiley Terms and Conditions for Use of Self-Archived Versions.*

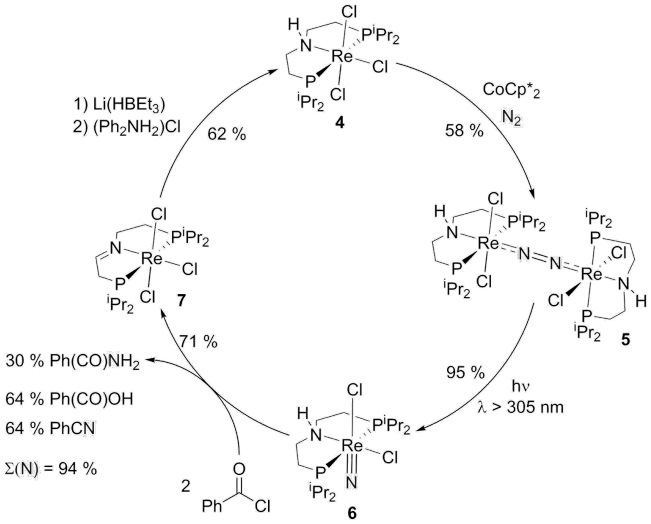

Scheme 2. Four step synthetic cycle for benzonitrile/benzamide synthesis.

Complex **4** was investigated by cyclic voltammetry (CV) under argon. Quasireversible, scan rate dependent reduction is observed at -1.84 V suggesting chloride loss on the CV time-scale.[16, 18] Chemical reduction with 1 equiv. $CoCp^*_2$ in tetrahydrofuran (THF) under an N_2 atmosphere (Scheme 2) gives an intensely blue product (**5**) in around 60% isolated yield. Complex **5** exhibits sharp and strongly shifted NMR signals suggesting an even-electron compound with a TIP contribution. Symmetric N_2 binding was confirmed by a single signal in the $^{15}N\{^1H\}$-NMR spectrum and a band at 1733 cm^{-1} ($^{15}N_2$-**5**: 1675 cm^{-1}) in the resonance Raman spectrum.[16] Two doublets in the $^{31}P\{^1H\}$-NMR spectrum (δ_P = -370.6/-380.4 ppm) with mutual *trans*-coupling ($^2J_{PP}$ = 237 Hz), eight ^1H NMR signals assignable to C*H*$_3$-groups and one amine N*H*-signal are in agreement with an N_2 bridged, dinuclear compound with C_2 symmetry, in analogy to **2**.[13b] Structural assignment as $[(\mu\text{-}N_2)\{ReCl_2(HPNP^{iPr})\}_2]$ was further substantiated by LIFDI mass spectrometry.

The molecular structure was confirmed by single crystal X-ray diffraction (Figure 1b).[16] The asymmetric unit features two octahedrally coordinated, linearly N_2-bridged Re-ions. The N–N bond length (1.169(5) Å) is slightly shorter compared with **2** (1.202(10) Å),[13b] indicating moderate N_2 activation in agreement with the Raman data. In contrast to **2**, the pincer nitrogen atoms are located *trans* to the N_2 bridge. The two $\{ReCl_2(HPNP^{iPr})\}$ fragments are twisted with respect to each other by 75.5° giving rise to idealized C_2 symmetry.

Unlike **2**, complex **5** shows remarkable thermal stability. No decomposition was observed over several days, even upon heating to 60 °C in THF. Thermal splitting was therefore examined computationally. Density functional theory (DFT) nicely reproduced the geometry of **5**.[16] In analogy to **2**,[13b] an electronic triplet configuration was obtained as the ground state. While any spin-orbit coupling effects likely present in this dimer are insufficiently described by DFT, the high kinetic barrier ($\Delta G^{\ddagger}_{298}$ = 41.8 kcal mol^{-1}) computed for thermal cleavage of **5** into the *trans*-dichloro nitride $[Re(N)(trans\text{-}Cl_2)(HPNP^{iPr})]$ (**6**^{trans}) is in accordance with experiment and contrasts with cleavage of **2** ($\Delta G^{\ddagger}_{298}$ = 26.9 kcal mol^{-1}).[13b] Interestingly, splitting of **5** into **6**^{trans} is almost thermoneutral (ΔG^{o}_{298} = 2.2 kcal mol^{-1}), as compared with strongly exergonic splitting of **2** into square-pyramidal **3** (ΔG^{o}_{298} = –40.3 kcal mol^{-1}).[13b] The less favorable thermochemistry for six-coordinate **6**^{trans} is attributed to the nitride *trans*-influence as expressed by a long Re–N_{PNP} bond (2.53 Å) and distorted pincer binding. Accordingly, relaxation to isomeric $[Re(N)(cis\text{-}Cl_2)(HPNP^{iPr})]$ (**6**) is strongly favorable (ΔG^{o}_{298} = -11.0 kcal mol^{-1} per molecule).

The striking thermal stability of **5** vs. **2** can be rationalized by qualitative molecular orbital (MO) considerations. Thermal cleavage of a linearly N_2 bridged M_2N_2 core proceeds via electron transfer into an MO with M–N–N–M σ-σ*-σ-character (Scheme 1) within a zig-zag shaped transition state (TS).[15,13b,19] Ligands *trans* to the N_2-bridge raise this MO in energy, thereby disfavoring N_2-splitting. A classic case for such geometry controlled reactivity might be the trisanilides $[(RArN)_3Mo]_2(N_2)]$,[20] which split into nitrides in contrast to analogous triamidoamine complexes.[3a]

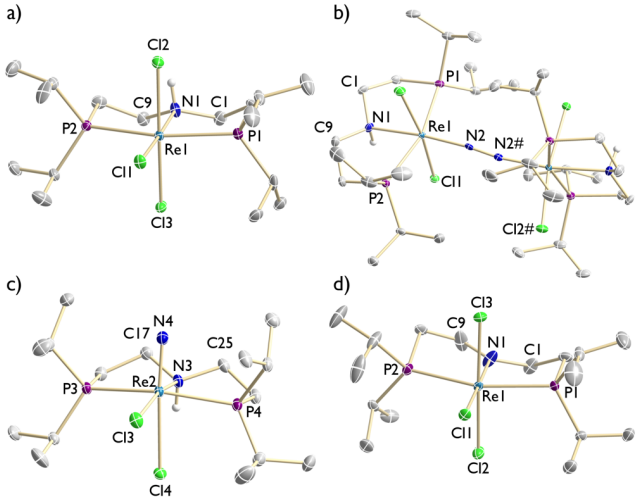

Figure 1. Molecular structures of **4** (a), **5** (b), **6** (c) and **7** (d) in the crystal obtained by single crystal X-ray diffraction. Hydrogen atoms were omitted for clarity except NH protons.[16]

To overcome kinetically hindered N_2-splitting we sought to populate N–N antibonding MOs by electronic excitation.[9, 21, 22] Photolysis of **5** in THF with a Xe arc lamp (λ > 305 nm) led to gradual color change to yellow over 2 h. ^{31}P and ^1H NMR spectra revealed the formation of *cis*-dichloro nitride complex **6** (Scheme 2) in 95 % spectroscopic yield upon comparison with an original sample.[16] Use of $^{15}N_2$-labelled **5** confirmed photolytic splitting of the N_2 ligand by $^{15}N\{^1H\}$ NMR spectroscopy. A quantum yield below 1 % was estimated by actinometry.[16] The configuration of **6** requires isomerization before or after N_2-splitting. Photolysis was therefore carried out in the presence of $NHex_4Cl$ (0-500 equiv.).[16] The independence of the reaction rate excludes isomerization by chloride (photo)dissociation prior to or as the rate determining step.

*This is the peer reviewed version of the following article: F. Schendzielorz et al., Angew. Chem. Int. Ed., **2019**, 58, 830-834, which has been published in final form at* **DOI**: 10.1002/anie.201812125. *This article may be used for non-commercial purposes in accordance with Wiley Terms and Conditions for Use of Self-Archived Versions.*

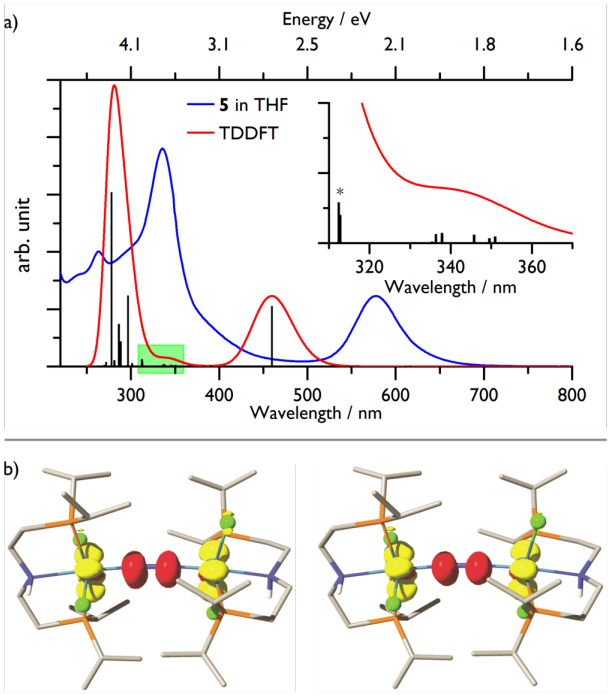

Figure 2. a) Comparison of the experimental (blue) and TDDFT-computed (red; S = 1; see ESI for details) electronic absorption spectra. The productive region for N_2 splitting is highlighted in the computed spectrum (green) and shown in the inset. b) Difference densities (loss in yellow, gain in red) of the two transitions marked with an asterisk in the inset.

Complex **5** exhibits two maxima above 300 nm in the UV-vis spectrum (λ_{max} = 336, ε = 38027 $M^{-1}cm^{-1}$; 578 nm, ε = 12294 $M^{-1}cm^{-1}$; Figure 2a). Wavelength selective photolysis indicates that the productive excitations for N_2-splitting are centered at a shoulder around 400 nm allowing for the use of a violet LED (390 nm) with the same yield.[16] TD-DFT reasonably well reproduced the electronic absorption spectrum (Figure 2a) with almost identical results for the open-shell singlet and triplet electronic structure configurations.[16] Computational evaluation of the highest intensity, yet unproductive absorptions indicates dominant contributions from transitions within the Re–N–N–Re π-manifold, such as (π^*-π-π^*)→(π^*-π^*-π^*) (calc: 278 nm, 4.46 eV) and (π-π^*-π)→(π^*-π-π^*) (calc: 460 nm, 2.70 eV). In contrast, two transitions in the productive spectral region (Figure 2a, inset) exhibit mainly (δ/δ^*)→(π^*-π^*-π^*) character (Figure 2b), implying considerably stronger Re→N_2 charge transfer. The weak oscillator strengths (f_{osc} ≤ 0.02) are in line with the low quantum yield obtained for photolytic splitting of the N_2 bridge.

While the excited state dynamics are not known at this point, the Re→N_2 MLCT character of these states is consistent with N_2 cleavage. Occupation of Re–N–N–Re (π^*-π^*-π^*)-MOs weakens N–N π-bonding and increases the flexibility of the Re_2N_2-core, which could facilitate cleavage via a zig-zag TS. At the same time, charge separation should enhance Re–N bonding. The spectral features of **5** resemble the visible region of [{Cp*(depf)Mo}$_2$(η_1:η_1:μ^2-N_2)] (depf = 1,1'-bisdi(ethylphosphino)ferrocene), which also splits into nitrides upon photolysis at 580 > λ > 400 nm.[22d]

In the solid state (Figure 1c),[16] **6** retains octahedral coordination with one significantly elongated Re–Cl bond (2.4309(7) Å *vs.* 2.6712(7) Å), reflecting the nitride *trans*-influence. In turn, the Re≡N bond (1.669(2)Å) is longer compared to five-coordinate [Re(N)Cl(*H*PNP^{tBu})]Cl (1.642(4) Å).[13a] Addition of NaBAr$^F_{24}$ (BAr$^F_{24}$ = tetrakis-(3,5-(trifluoromethyl)phenyl)borate) to **6** in THF results in two new ^{31}P NMR signals that are assigned to two isomers of [Re(N)Cl(*H*PNP^{iPr})]$^+$.[16] In turn, **6** is fully restored upon addition of NHex$_4$Cl. Hence, six-coordinate [Re(N)Cl$_2$(*H*PNP^{iPr})] is the dominant species in solution. Reduced steric shielding facilitates chloride coordination and thereby weakening of metal nitride bonding.

Heating of **6** with PhC(O)Cl (2 equiv.) at 80 °C in 1,4-dioxane over 15 h gives a new rhenium species (**7**) in 71 % yield (Scheme 2). Paramagnetically shifted and sharp NMR signals support reduction to Re^{III}. Two chemically inequivalent P-atoms (δ_P = -1592.6, -1615.5 ppm; $^2J_{PP}$ = 248 Hz) and the ^{1}H and ^{13}C NMR signatures are in agreement with pincer oxidation to an imine ligand.[16] Formation of [ReCl$_3$(P=NP^{iPr})] (P=NP^{iPr} = N(CHCH$_2$*i*Pr$_2$)(CH$_2$CH$_2$*i*Pr$_2$)) was confirmed by LIFDI-MS and comparison with an authentic sample.[16] Crystallographic characterization (Figure 1d) evidences nitride transfer and pincer dehydrogenation.[16] Two products account for 94 % of the nitride ligand, i.e. benzamide (30 %), and benzonitrile (64 % with equimolar benzoic acid), respectively. PhCN and PhCO$_2$H are products from the reaction of benzamide with benzoyl chloride,[23] supporting that PhC(O)NH$_2$ is the immediate product of nitride benzoylation and 2e$^-$/2H$^+$-transfer from the pincer ligand. Related reactivity was observed for [Ru(N)(*H*PNP^{tBu})]$^+$, which gives [Ru(NH$_3$)(O$_2$CPh)(P=NP^{tBu})]$^+$ upon reaction with *para*-methoxy benzoic acid.[24] However, in that case azide was used as nitrogen source rather than N_2.

Next, re-reduction of the imine pincer ligand was examined to evaluate the amine/imine redox couple as cooperating ligand reservoir for 2e$^-$/2H$^+$ proton coupled electron transfer (PCET). **7** does not react with H_2 under thermal or photolytic conditions. However, chemical reduction is possible with stepwise addition of Li[HBEt$_3$] and diphenylammonium chloride (Scheme 2). On this route, **4** is obtained in 62 % spectroscopic yield due to the formation of rhenium hydrides as byproducts, which reform **7** upon hydrolytic quenching.

We therefore turned to electrochemical regeneration of **4**. The CV of **7** exhibits quasi-reversible reduction at -1.70 V. Titrating in benzoic acid (0-15 eq.; Figure 3a) results in a pronounced increase of the cathodic current and buildup of a second, quasi-reversible reductive feature at -1.84 V, which is assigned to parent **4**. The strong increase of the first wave is indicative of multielectron reduction in the presence of acid. In fact, the viable intermediate [ReCl$_3$(PNP^{iPr})] (**8**) exhibits a quasi-reversible reduction at -1.16 V,[16] confirming a potential inversion after the first e$^-$/H$^+$-transfer to **7**. The electrochemical data in the presence of acid is therefore rationalized with two subsequent PCET steps at around –1.7 V that regenerate **4**.

Controlled potential electrolysis (CPE) of **7** at the half peak potential of the first reduction feature (*E* = -1.65 V) did not give appreciable amounts of **4** in the presence of benzoic acid (10 eq). 2,6-Dichlorophenol (DCP) was therefore employed, which exhibits about same pK_a as benzoic acid (pK_a^{THF} = 25.1)[25] yet a conjugate base that is less prone to metal coordination. In fact,

*This is the peer reviewed version of the following article: F. Schendzielorz et al., Angew. Chem. Int. Ed., **2019**, 58, 830-834, which has been published in final form at* **DOI**: 10.1002/anie.201812125. *This article may be used for non-commercial purposes in accordance with Wiley Terms and Conditions for Use of Self-Archived Versions.*

bulk electrolysis of **7** at E = -1.65 V in the presence of DCP (10 eq.) for 7 h results in full consumption of **7** and formation of **4** as the only electroactive species. ^{1}H NMR spectroscopy confirmed a yield of 99 % and coulometry the transfer of 1.96 e$^-$ per **7**.

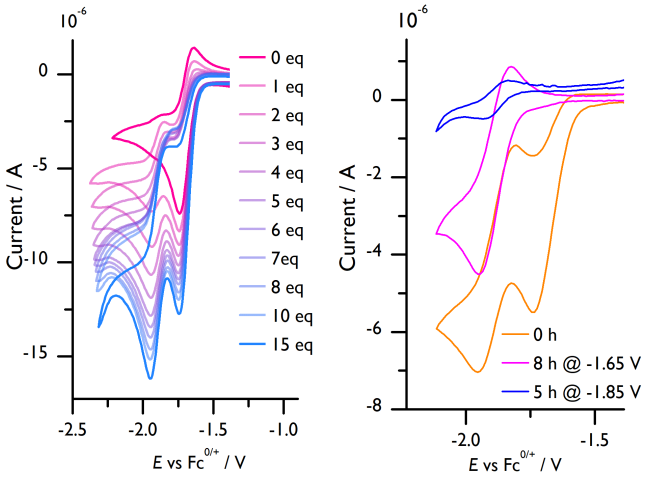

Figure 3. *Left*: CV of **7** in presence of 0–15 eq. benzoic acid. *Right*: CV of **7** with 10 eq 2,6-dichlorophenol under N_2 before CPE (orange), after 8 h CPE at -1.65 V (pink) and after subsequent 5 h CPE at -1.85 V (blue).

The quantitative regeneration of **4** motivated the examination of *in situ* electrochemical N_2 activation. In a CPE experiment, **7** was electrolyzed with DCP (10 eq.) under N_2 for 8 h at E = -1.65 V, followed by 5 h at E = -1.85 V, i.e. the half potential of the reduction of **4** (Figure 3b). Overall, 3.32 e$^-$ per Re atom were transferred. Formation of complex **5** during the second electrolysis step was indicated by the deep blue color and confirmed by ^{1}H and ^{31}P{^{1}H} NMR spectroscopy. UV/Vis spectroscopic quantification gave a yield around 70 % (Scheme 3). In situ photolysis (390 nm LED) of this mixture revealed N_2 splitting to nitride **6** as the only detectable product by ^{31}P{^{1}H} and ^{1}H NMR spectroscopy. However, the yield in **6** dropped to 14 % with respect to parent **7**, i.e. considerably lower compared to photolysis of isolated **5**.

In summary, a three-step cycle for the generation of benzamide/benzonitrile from N_2 in overall 61 % yield (with respect to N) was established that relies on electrochemical N_2 activation, photochemical splitting into nitrides and thermal nitrogen transfer (Scheme 3). This model reveals some basic principles in comparison to our previously reported system.[7,13] Use of a sterically less encumbered pincer ligand stabilizes higher coordination numbers. In consequence, thermal N_2 splitting becomes less favorable which can be overcome by photolysis with visible light. Based on the experimental and theoretical data, the photochemical reactivity is associated with the population of a dissociative state with Re→N_2 MLCT character. The higher coordination number weakens nitride bonding, thus enabling the use of a weaker electrophile than alkyl triflates. Importantly, the cooperating pincer ligand serves as a reservoir for nitrogen hydrogenolysis upon 2e$^-$/2H$^+$-PCET and electrochemical re-hydrogenation. Our results demonstrate how metal-ligand cooperativity and photo- and electrochemical approaches can facilitate the design of platforms for N_2-fixation.

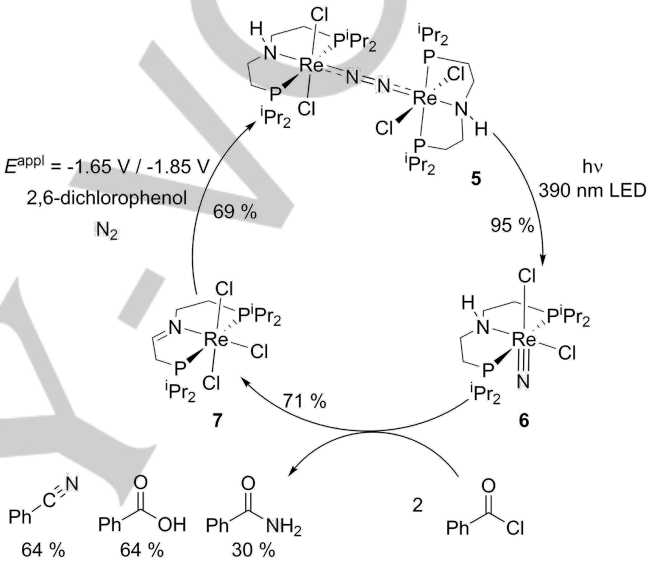

Scheme 3. Optimized, three-step synthetic cycle.

Acknowledgements

This work was supported by the European Research Council (ERC Consolidator Grant Agreement 646747, grant holder S.Sch.). V.K. acknowledges a 50th Anniversary Prize Fellowship from the University of Bath and its Balena High Performance Computing (HPC) Service. The authors thank Dr. C. Volkmann for solving the crystal structure of complex **8**.

Keywords: Nitrogen Fixation • Rhenium • Pincer Ligand • Photochemistry • Electrochemistry

[1] S. L. Foster, S. I. Perez Bakovic, R. D. Duda, S. Maheshwari, R. D. Milton, S. D. Minteer, M. J. Janik, J. N. Renner, L. F. Greenlee, *Nat. Catal.* **2018**, *1*, 490.

[2] B. M. Lindley, A. M. Appel, K. Krogh-Jespersen, J. M. Mayer, A. J. M. Miller, *ACS Energy Lett.* **2016**, *1*, 698.

[3] (a) R. Schrock, *Angew. Chem., Int. Ed.* **2008**, *47*, 5512. (b) H. Tanaka, Y. Nishibayashi, K. Yoshizawa, *Acc. Chem. Res.* **2016**, *49*, 987. (c) R. J. Burford, M. D. Fryzuk, *Nat. Rev. Chem.* **2017**, *1*, 00261.

[4] (a) C. J. Pickett, J. Talarmin, *Nature* **1985**, 317, 652. (b) J. Y. Becker, B. Posin, *J. Electroanal. Chem. Interfacial Electrochem.* **1988**, *250*, 385. (c) J. Y. Becker, S. Avraham, B. Posin, *J. Electroanal. Chem. Interfacial Electrochem.* **1987**, *230*, 143. (d) N. P. Luneva, S. A. Mironova, A. E. Shilov, M. Y. Antipin, Y. T. Struchkov, *Angew. Chem., Int. Ed. Engl.* **1993**, *32*, 1178. (e) T. Munisamy, R. R. Schrock, *Dalton Trans.* **2012**, *41*, 130. (f) T. J. Del Castillo, N. B. Thompson, J. C. Peters, *J. Am. Chem. Soc.* **2016**, *138*, 5341. (g) M. J. Chalkley, T. J. Del Castillo, B. D. Matson, J. C. Peters, *J. Am. Chem. Soc.* **2018**, *140*, 6122.

[5] Y. Tanabe, Y. Nishibayashi, *Coord. Chem Rev.* **2013**, *257*, 2551.

*This is the peer reviewed version of the following article: F. Schendzielorz et al., Angew. Chem. Int. Ed., **2019**, 58, 830-834, which has been published in final form at* **DOI**: 10.1002/anie.201812125*. This article may be used for non-commercial purposes in accordance with Wiley Terms and Conditions for Use of Self-Archived Versions.*

[6] (a) J. S. Figueroa, N. A. Piro, C. R. Clough, C. C. Cummins, *J. Am. Chem. Soc.* **2006**, *128*, 940. (b) J. J. Curley, E. L. Sceats, C. C. Cummins, *J. Am. Chem. Soc.* **2006**, *128*, 14036.

[7] (a) I.Klopsch, M. Kinauer, M. Finger, C. Würtele, S. Schneider, *Angew. Chem. Int. Ed.* **2016**, *55*, 4786. (b) I. Klopsch, F. Schendzielorz, C. Volkmann, C. Würtele, S. Schneider, *Z. Anorg. Allg. Chem.* **2018**, *644*, 916.

[8] M. M. Guru, T. Shima, Z. Hou, *Angew. Chem. Int. Ed.* **2016**, *128*, 12504.

[9] A. J. Keane, W. S. Farrell, B. L. Yonke, P. Y. Zavalij, L. R. Sita, *Angew. Chem. Int. Ed.* **2015**, *54*, 10220.

[10] Q. Liao, A. Cavaillé, N. Saffon-Merceron, N. Mézailles, *Angew. Chem. Int. Ed.* **2016**, *128*, 11378.

[11] L. M. Duman, L. R. Sita, *J. Am. Chem. Soc.* **2017**, *139*, 17241.

[12] M. F. Espada, S. Bennaamane, Q. Liao, N. Saffon-Merceron, S. Massou, E. Clot, N. Nebra, M. Fustier-Boutignon, N. Mézailles, *Angew. Chem. Int. Ed.* **2018**, *130*, 13047.

[13] (a) I. Klopsch, M. Finger, C. Würtele, B. Milde, D. B. Werz, S. Schneider, *J. Am. Chem. Soc.* **2014**, *136*, 6881. (b) B. M. Lindley, R. S. van Alten, M. Finger, F. Schendzielorz, C. Würtele, A. J. M. Miller, I. Siewert, S. Schneider, *J. Am. Chem. Soc.* **2018**, *140*, 7922.

[14] G. Silantyev, M. Förster, B. Schluschaß, J. Abbenseth, C. Würtele, C. Volkmann, M.C. Holthausen, S. Schneider, *Angew. Chem. Int. Ed.* **2017**, *56*, 5872.

[15] I. Klopsch, E.Y. Yuzik-Klimova, S. Schneider, *Top. Organomet. Chem.* **2017**, *60*, 71.

[16] For synthetic, spectroscopic, computational and crystallographic details see Electronic Supporting Information (ESI).

[17] (a) J. Chatt, G. J. Leigh, D. M. P. Mingos, *J. Chem. Soc. (A)* **1969**, 1674. (b) J. Abbenseth, M. Diefenbach, S. C. Bete, C. Würtele, C. Volkmann, S. Demeshko, M. C. Holthausen, S. Schneider, *Chem. Commun.* **2017**, *53*, 5511.

[18] All electrochemical data is reported *vs.* $FeCp_2^+/FeCp_2$.

[19] C. E. Laplaza, M. J. A. Johnson, J. C. Peters, A. L. Odom, E. Kim, C. C. Cummins, G. N. George, I. J. Pickering, *J. Am. Chem. Soc.* **1996**, *118*, 8623.

[20] C. E. Laplaza, C. C. Cummins, *Science* **1995**, *268*, 861.

[21] V. Krewald, *Dalton Trans.* **2018**, *47*, 10320.

[22] (a) J. J. Curley, T. R. Cook, S. Y. Reece, P. Müller, C. C. Cummins, *J. Am. Chem. Soc.* **2008**, *130*, 9394. (b) H. Kunkely, A. Vogler, *Angew. Chem. Int. Ed.* **2010**, *49*, 1591. (c) A. S. Huss, J. J. Curley, C. C. Cummins, D. A. Blank, *J. Phys. Chem. B* **2013**, *117*, 1429. (d) T. Miyazaki, H. Tanaka, Y. Tanabe, M. Yuki, K. Nakajima, K. Yoshizawa, Y. Nishibayashi, *Angew. Chem. Int. Ed.* **2014**, *53*, 11488. (e) L. M. Duman, W. S. Farrell, P. Y. Zavalij, L. R. Sita, *J. Am. Chem. Soc.* **2016**, *138*, 14856.

[23] D. Davidson, H. Skovronek, *J. Am. Chem. Soc.* **1958**, *80*, 376.

[24] (a) B. Askevold, J. Torres Nieto, S. Tussupbayev, M. Diefenbach, E. Herdtweck, M. C. Holthausen, S. Schneider, *Nature. Chem.* **2011**, *3*, 532. (b) B. M. Lindley, Q. J. Bruch, P. S. White, F. Hasanayn, A. J. M. Miller, *J. Am. Chem. Soc.* **2017**, *139*, 5305.

[25] a) D. Barrón, J. Barbosa, *Anal. Chim. Acta* **2000**, *403*, 339. b) D. Barrón, J. Barbosa, *Anal. Chim. Acta* **1992**, *265*, 157.

WILEY-VCH

*This is the peer reviewed version of the following article: F. Schendzielorz et al., Angew. Chem. Int. Ed., **2019**, 58, 830-834, which has been published in final form at* **DOI**: 10.1002/anie.201812125*. This article may be used for non-commercial purposes in accordance with Wiley Terms and Conditions for Use of Self-Archived Versions.*

Entry for the Table of Contents

COMMUNICATION

Cooperative Fixation: N_2 fixation to benzonitrile and benzamide is reported within a three-step cycle that utilizes electrochemical reduction, photochemical N_2 splitting and thermal *N*-transfer with benzoylchloride. Product formation is enabled by cooperativity of the functional pincer ligand, which serves as a $2H^+/2e^-$ reservoir.

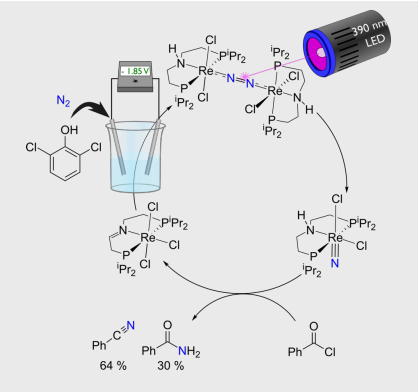

F. Schendzielorz, M. Finger, J. Abbenseth, C. Würtele, V. Krewald, S. Schneider**

Page No. – Page No.

Metal-Ligand Cooperative Synthesis of Benzonitrile via Electrochemical Reduction and Photolytic Splitting of Dinitrogen

WILEY-VCH